International Current Journal of Engineering and Science (ICJES)
Volume 4, Issue 12, pp 1-6, December-2025
ISSN (Online): 2583-7257
Article DOI: https://doi.org/10.47001/ICJES/2025.412001

Failure Analysis and Design Optimization of One-Third Tubular Plate Using Finite Element Analysis

[1]Rionditya Soni Bagastomo, [2]*Rifky Ismail, [3]Ismoyo Haryanto

[1,2,3]Department of Mechanical Engineering, Diponegoro University, Jl. Prof. Soedarto, No.13, Tembalang, Semarang, 50275, Central Java, Indonesia
[1]Department of Application Engineering, PT Arisma Data Setia, Jl. Graha Anggrek Mas No. A18, Pagerwojo, Sidoarjo, 61252, East Java, Indonesia
[2]Center for Biomechanics, Biomaterial, Biomechatronics, and Biosignal Processing (CBIOM3S), Diponegoro University,Jl. Prof. Soedarto No.13, Tembalang, Semarang, 50272, Central Java, Indonesia
*Corresponding Author's E-mail: r.ismail.undip@gmail.com

Abstract **- Fibula fractures are common injuries often treated through internal fixation; however, post-operative mechanical failure of implants remains a significant clinical challenge. This study aims to analyze the causes of implant failure in a clinical case and optimize the design thickness using Finite Element Analysis (FEA). The study simulates a one-third tubular plate made of Stainless Steel 316L with thickness variations of 2 mm, 2.5 mm, and 3 mm using a four-point bending test scheme. Simulation results indicate that the standard 2 mm implant has critical structural limitations with a maximum load capacity of only 181.23 N, validating the cause of failure due to excessive functional loads. Conversely, thickness modification proved to significantly enhance mechanical performance: the 2.5 mm model increased load capacity by 50.1%, while the 3 mm model recorded a superior increase of 118.2% with a load capacity of up to 395.52 N. It is concluded that the 3 mm thickness variation is the optimal design, offering the best safety factor and stiffness to ensure fixation stability and prevent recurrent failure.**

Keywords: Finite element analysis, Biomechanics, One-third tubular plate, Bending test, Fibula fracture.

I. INTRODUCTION

Fractures of the fibula dominate lower extremity injury statistics and are classified as musculoskeletal disorders with a high frequency of occurrence [1]. Surgical intervention via internal fixation, utilizing a combination of plates and screws, is often the primary choice to ensure stability of the fracture area during the recovery period [2]. Nevertheless, post-operative mechanical complications, such as implant deformation or breakage, remain serious obstacles and persistent challenges in modern orthopedic practice [3].

This research was initiated based on clinical observations in 2023 regarding a 39-year-old male patient who suffered a fibula fracture due to a traffic accident. Following the surgical installation of a one-third tubular plate fixation, radiological monitoring after two months revealed structural failure in the form of a broken implant at the fracture site. This phenomenon indicates that the load capacity of the implant design was insufficient to withstand the mechanical forces acting during the patient's healing phase [4].

To mitigate the risk of implant failure or refracture in the future, a comprehensive evaluation of the implant's mechanical integrity is crucial. Therefore, this research focuses on optimizing implant thickness through a Finite Element Analysis (FEA) approach. The use of this computational method is considered strategic due to its reliability in projecting stress distribution and the biomechanical response of orthopedic implants as a pre-clinical evaluation step [5].

II. METHODOLOGY

The evaluation of implant mechanical performance in this study was conducted through computational simulation using Finite Element Analysis (FEA). The research procedure was arranged systematically, starting from geometry model construction, material parameter definition, discretization (meshing), to the application of boundary conditions aligned with standard testing protocols for bone plates.

2.1 Geometry Design and Material

The object of study, a one-third tubular plate with an eight-hole configuration, was modeled in three dimensions using SOLIDWORKS 2025 software, as shown in Figure 1. For design optimization purposes, the plate geometry was developed in three different thickness variations. The first model features a thickness of 2 mm, representing the actual condition in the clinical case, while the other two models were

© 2025 ICJES All Rights Reserved

International Current Journal of Engineering and Science (ICJES)
Volume 4, Issue 12, pp 1-6, December-2025
ISSN (Online): 2583-7257
Article DOI: https://doi.org/10.47001/ICJES/2025.412001

modified to 2.5 mm and 3 mm as parameters for mechanical strength comparison.

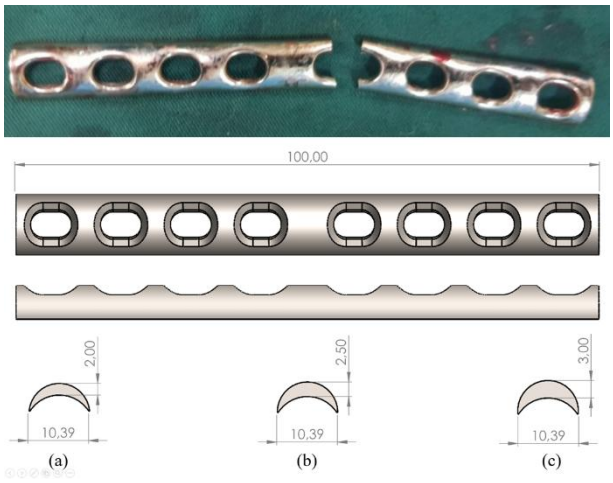

Figure 1: Clinical failure of the implant and the geometric models of the 8-hole one-third tubular plate with thickness variations (a) 2.00 mm (b) 2.50 mm and (c) 3.00 mm

The material used in this simulation is Stainless Steel 316L referring to the ASTM F138 standard [6], which is known for its superior mechanical properties and good corrosion resistance for engineering applications [7]. The mechanical properties refer to experimental data from tensile tests. Material characteristics are visualized in the true stress-strain graph as seen in Figure 2. Based on this data, the material definition in the FEA solver was set using the von Mises plasticity criterion to simulate plastic deformation response.

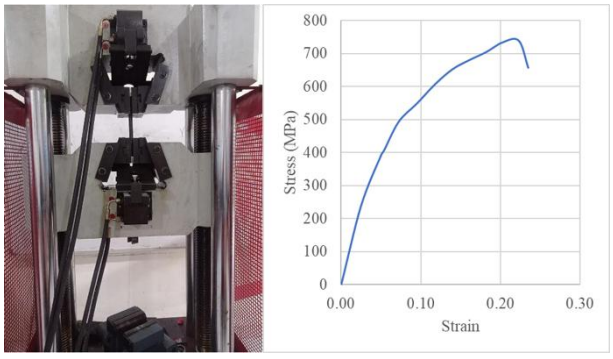

Figure 2: Tensile testing equipment and the true stress-strain graph of Stainless Steel 316L

2.2 Testing Configuration and Convergence Study

Implant strength evaluation was performed through simulation using a four-point bending scheme. This analysis is defined as a non-linear static study to accommodate the plastic deformation behavior of the material and large geometric changes. The testing configuration was specifically arranged to represent loading conditions relevant to the case studied. The determination of support positions and load application areas was applied to the finite element model as illustrated in detail in Figure 3.

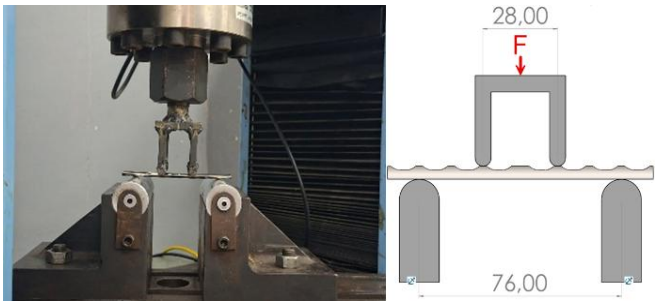

Figure 3: Boundary condition configuration for the four-point bending test in the FEA simulation

The loading mechanism in this simulation was applied using the displacement control method. To ensure the accuracy and independence of simulation results regarding element size, a mesh convergence study was conducted [8]. The element size iteration process was carried out gradually, and the final mesh size was determined when the deviation of the maximum von Mises stress value between the current and previous iterations reached stability with a difference below 2% [9]. As an illustration of these iteration stages, a visual comparison of element size distribution between coarse mesh and fine mesh configurations is displayed in Figure 4.

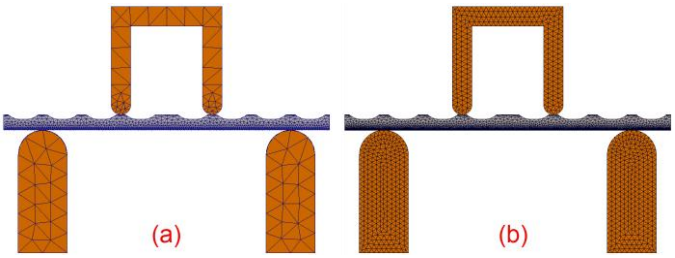

Figure 4: Comparison of mesh density for the convergence study showing (a) the initial Coarse Mesh (b) the refined Fine Mesh

III. RESULTS AND DISCUSSIONS

This chapter presents quantitative data obtained from Finite Element Analysis on three implant model variations with thicknesses of 2 mm, 2.5 mm, and 3 mm. Data is presented descriptively, covering stress distribution contours, deformation visualization, and load capacity curves, which are then comprehensively analyzed to determine the optimal design.

3.1 Von Mises Stress Distribution

To evaluate the relative durability between models, the simulation was conducted by applying a constant load of 181.23 N to all three variations. This load value was

© 2025 ICJES All Rights Reserved

International Current Journal of Engineering and Science (ICJES)
Volume 4, Issue 12, pp 1-6, December-2025
ISSN (Online): 2583-7257
Article DOI: https://doi.org/10.47001/ICJES/2025.412001

determined based on the peak load point (ultimate load) of the 2 mm plate, representing the failure limit of the weakest model.

Visualization of von Mises stress contours under these loading conditions is presented in Figure 5. Based on the visualization results, significant differences in stress distribution are observed despite identical loading. In Model A (2 mm), the area around the central screw holes (holes 4 and 5) is dominated by high stress concentrations approaching the material's maximum limit. Conversely, in Model B (2.5 mm), stress intensity begins to decrease, marked by a change in color gradation in the critical area, with a recorded maximum stress value of 425.98 MPa. The most drastic stress reduction is seen in Model C (3 mm), where the central plate area is dominated by blue, indicating that the occurring stress is much lower, at 409.44 MPa, despite sustaining the same load magnitude.

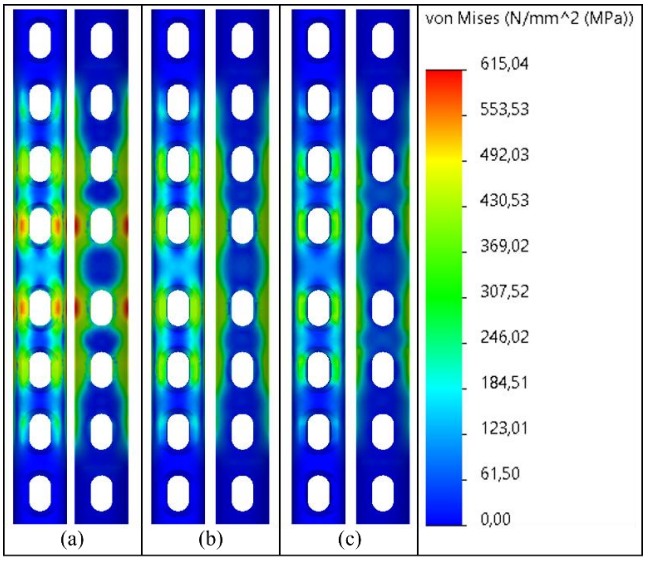

Figure 5: Von Mises stress contours across the different plate thicknesses of (a) 2 mm (b) 2.5 mm (c) 3 mm

3.2 Deformation (Displacement)

In addition to stress analysis, the structural response to critical loads was also evaluated through the total displacement parameter to assess the relative stiffness between models. Visualization of displacement distribution when subjected to a static load of 181.23 N is shown in Figure 6. Simulation results show a very striking difference in mechanical behavior due to thickness variation.

Under these loading conditions, Model A (2 mm) experienced structural failure in the form of extreme deflection reaching a maximum value of 10.15 mm, characterized by red distribution in the significantly curved central plate area. This deflection magnitude indicates a total loss of structural stiffness. Conversely, the thickness increase in Model B (2.5 mm) and Model C (3 mm) provided a drastic impact on stiffness. Both models demonstrated very high deformation resistance, visualized by the dominance of blue across the entire plate surface. Quantitatively, Model B (2.5 mm) experienced only micro-deflection of 1.60 mm, and Model C (3 mm) recorded the lowest deflection of 0.63 mm. This proves that at the same load where the 2 mm plate experienced total deformation failure, the plates with 2.5 mm and 3 mm thickness still maintained their form integrity.

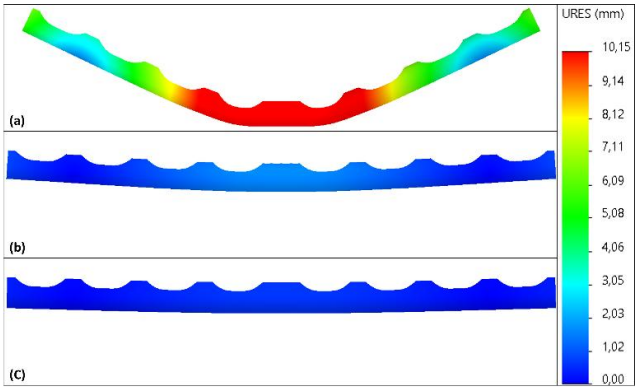

Figure 6: Displacement distribution contours for plate thicknesses of (a) 2 mm, (b) 2.5 mm, and (c) 3 mm

3.3 Load Capacity (Force-Displacement)

The mechanical characteristics of the implant up to the failure limit were comprehensively analyzed using Force-Displacement and Stress-Displacement curves presented in Figure 7 and Figure 8. These curves record the implant's reaction force response to the applied displacement until reaching the failure point or load drop. Based on the graphs, a significant difference in Ultimate Load capacity between thickness variations is observed.

Model A (2 mm) showed the weakest mechanical response, where the force curve began to flatten in the plastic phase and reached a peak point (maximum load) of only 181.23 N at a displacement of 10.15 mm. After this point, the implant was no longer able to withstand additional load. The increase in thickness in Model B (2.5 mm) resulted in a tangible increase in load capacity, with a maximum load recorded at 272.02 N at a displacement of 10.07 mm. The highest mechanical performance was demonstrated by Model C (3 mm), which was capable of withstanding loads up to 395.52 N before experiencing a force drop at a displacement of 8.97 mm. Besides having the largest load capacity, the curve for Model C also showed a steeper force increase gradient in the initial phase, indicating higher structural stiffness compared to the other two models.

© 2025 ICJES All Rights Reserved

International Current Journal of Engineering and Science (ICJES)
Volume 4, Issue 12, pp 1-6, December-2025
ISSN (Online): 2583-7257
Article DOI: https://doi.org/10.47001/ICJES/2025.412001

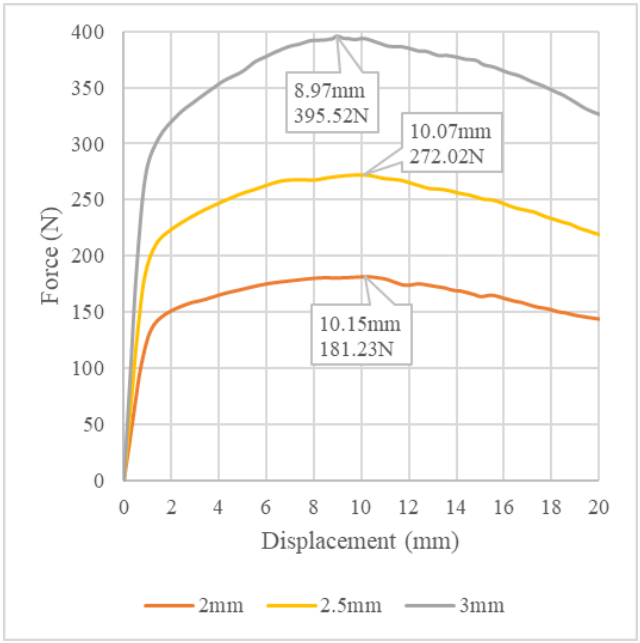

Figure 7: Comparison of force-displacement relationships for the three implant models

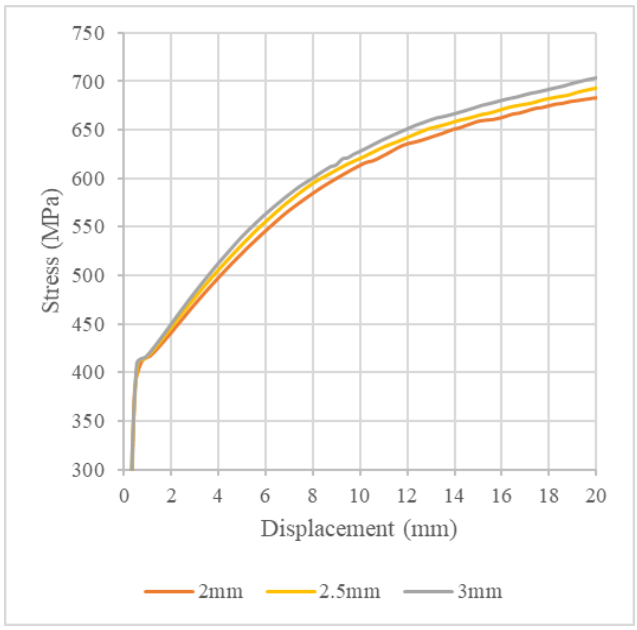

Figure 8: Comparison of stress-displacement relationships for the three implant models

3.4 Discussion

This sub-chapter analyzes the correlation between stress data, deformation, and load capacity to synthesize findings regarding the implant's biomechanical performance. A summary of key parameters from simulation results is displayed in Table 1.

Table 1: FEA Simulation Results on Implant Thickness Variations

Model Variation	Stress at Peak Load (MPa)	Displacement at Peak Load (mm)	Ultimate Force (N)	Capacity Increase (%)
Model A (2 mm)	615.04	10.15	181.23	-
Model B (2.5 mm)	621.06	10.07	272.02	+50.1%
Model C (3 mm)	613.98	8.97	395.52	+118.2%

In-depth analysis of the data in Table 1 reveals the root cause of failure in the standard 2 mm implant. The maximum load capacity of 181.23 N in Model A is considered critical for applications in the lower extremities. In clinical scenarios, patient physiological loads can often approach or exceed this figure. When the external load exceeds 181.23 N, the 2 mm implant will undergo permanent plastic failure, as indicated by the high deformation (10.15 mm) at that peak point. This validates the clinical event in the 2023 patient, where the implant failed to maintain its integrity due to functional loads exceeding the plate's structural capacity.

Conversely, design modification through increased thickness proved to provide exponential performance improvement. Model B (2.5 mm) provided a load capacity increase of 50.1%, but Model C (3 mm) offered a far superior increase of 118.2% compared to the standard model. With a load-bearing capacity of up to 395.52 N, Model C possesses a much larger Safety Factor. This means that if a patient loads the leg with a force of 181 N (the breaking point of the old implant), Model C is still far below its maximum limit and remains in a safe elastic phase. Furthermore, the displacement value at peak load for Model C (8.97 mm), which is lower compared to other models, indicates that this implant is more rigid and stable. Therefore, based on the synthesis of strength and stiffness data, the 3 mm thickness variation is recommended as the best design solution to prevent recurrent failure.

The simulation validation achieved in this research aligns with current literary developments regarding implant reliability analysis. The obtained data reinforces previous studies [10] that validate the efficacy of the finite element

© 2025 ICJES All Rights Reserved

International Current Journal of Engineering and Science (ICJES)
Volume 4, Issue 12, pp 1-6, December-2025
ISSN (Online): 2583-7257
Article DOI: https://doi.org/10.47001/ICJES/2025.412001

approach as a method for predicting orthopedic implant durability. The reliability of this method is also proven consistent across various biomechanical applications, such as in bionic feet [11], ESAR prosthetics [12], bionic hands [13], [14], and hip implants [15], [16]. Collectively, this underscores the vital role of finite element simulation as an accurate pre-production evaluation tool to ensure the mechanical integrity and safety of biomedical designs.

IV. CONCLUSION

Based on the Finite Element Analysis performed on the one-third tubular plate implant, this research successfully confirmed the cause of mechanical failure in the studied clinical case. Simulation results indicate that the standard implant with a thickness of 2 mm has critical structural limitations with a maximum load capacity of only 181.23 N, which is deemed inadequate to withstand lower extremity functional loads. The thickness modification strategy proved effective in exponentially improving mechanical performance, where Model B (2.5 mm) provided a capacity increase of 50.1%, and Model C (3 mm) recorded a superior increase of 118.2% with the ability to withstand loads up to 395.52 N. Therefore, the 3 mm thickness variation is established as the optimal design as it offers the best combination of a high Safety Factor and adequate structural stiffness to ensure fixation stability and prevent the risk of recurrent failure in the future.

ACKNOWLEDGEMENT

The authors would like to thank Diponegoro University for providing laboratory facilities for experimental validation, and PT Arisma Data Setia for technical assistance in conducting the Finite Element Analysis (FEA). The resource support provided by both institutions was vital for the smooth execution and completion of this research.

REFERENCES

[1] C. M. Court-Brown and B. Caesar, “The epidemiology of adult fractures: A review,” *Injury*, vol. 37, no. 8, pp. 691–697, Aug. 2006.

[2] R. E. Buckley, C. G. Moran, and T. Apivatthakakul, AO Principles of Fracture Management. *New York, NY, USA: Thieme*, 2017.

[3] A.H. M. Aziz et al., “Implant failure in fracture fixation: A systematic review,” *Journal of Orthopaedic Surgery and Research*, vol. 14, no. 1, p. 123, 2019.

[4] M. A. Haque and M. S. Islam, “Failure analysis of a stainless steel orthopaedic implant,” *Journal of Failure Analysis and Prevention*, vol. 15, no. 2, pp. 209–216, 2015.

[5] B. Y. Li et al., “Finite element analysis of bone plates used for fixation of mandibular fractures,” *Journal of Biomechanics*, vol. 44, no. 10, pp. 1956–1961, 2011.

[6] ASTM International, “Standard Specification for Wrought 18 Chromium-14 Nickel-2.5 Molybdenum Stainless Steel Bar and Wire for Surgical Implants (UNS S31673),” *ASTM F138-19, West Conshohocken, PA*, 2019.

[7] N. Alias, S. A. Bakar, and H. S. Intan, "Analysis of Intermetallic Compounds in 316L SS during the Electro Deposition Process Using Coating of Al-Zn-Mg-Si Alloy," *International Current Journal of Engineering and Science (ICJES)*, vol. 3, no. 11, pp. 22-28, Nov. 2024.DOI: https://doi.org/10.47001/ICJES/2024.311004

[8] O. C. Zienkiewicz, R. L. Taylor, and J. Z. Zhu, The Finite Element Method: Its Basis and Fundamentals, *7th ed. Oxford, UK: Butterworth-Heinemann*, 2013.

[9] K. J. Bathe, Finite Element Procedures, *2nd ed. Watertown, MA, USA: Klaus-Jurgen Bathe*, 2014.

[10] Haryanto, R. S. Bagastomo, R. Ismail, J. P. Siregar, and T. Cionita, "Computational Assessment of Orthopedic Implant Durability Using Finite Element Analysis," *Adv. Sustain. Sci. Eng. Technol.*, vol. 7, no. 3, Art. no. 02503028, 2025. DOI: 10.26980/asset.v7i3.2503028

[11] H. Prawibowo, F. T. Putri, R. Ismail, et al., "Finite Element Analysis on a Bionic Foot Prosthesis Model during Walking Gait Phases," *in 2023 IEEE Int. Biomed. Instrum. Technol. Conf. (IBITeC)*, 2023, pp. 98-102. DOI: 10.1109/IBITeC58648.2023.10428529

[12] A.F. Istiqomah, R. Ismail, D. F. Fitriyana, et al., "Design and Analysis of The Energy Storage and Return (ESAR) Foot Prosthesis Using Finite Element Method," *J. Biomed. Sci. Bioeng.*, vol. 1, no. 2, pp. 59-64, 2022. DOI: 10.14710/jbiomes.2021.v1i2.59-64

[13] G. P. Annanto, I. Haryanto, and R. Ismail, "A Computational Stress Analysis of Active Prosthetic Hand “Asto Hand V4” for the Loaded Hook Position," *in 2021 IEEE Int. Biomed. Instrum. Technol. Conf. (IBITeC)*, 2021, pp. 65-69. DOI: 10.1109/IBITeC53045.2021.9649122

[14] G. P. Annanto, R. Ismail, I. Haryanto, et al., "Numerical Analysis of Stress and Displacement on the Index Finger of the Prosthetic Hand Due to Hook Position," *AIP Conf. Proc.*, vol. 2187, no. 1, Art. no. 020034, 2019. DOI: 10.1063/1.5138290

[15] R. B. Taqriban, R. Ismail, J. Jamari, and A. P. Bayuseno, "Finite Element Analysis of Artificial Hip Joint Implant Made from Stainless Steel 316L," *Bali Med. J.*, vol. 10, no. 1, pp. 448-452, 2021. DOI: 10.15562/bmj.v10i1.2366

© 2025 ICJES All Rights Reserved

International Current Journal of Engineering and Science (ICJES)

Volume 4, Issue 12, pp 1-6, December-2025

ISSN (Online): 2583-7257

Article DOI: https://doi.org/10.47001/ICJES/2025.412001

[16] R. B. Taqriban, R. Ismail, J. Jamari, and A. P. Bayuseno, "Computational Analysis of Different Designed Hip Joint Prostheses Using Finite Element Method," *in 2020 7th Int. Conf. Inf. Technol. Comput. Electr. Eng. (ICITACEE)*, 2020, pp. 28-32. DOI: 10.1109/ICITACEE50144.2020.9239113.

Citation of this Article:

Rionditya Soni Bagastomo, Rifky Ismail, Ismoyo Haryanto. (2025). Failure Analysis and Design Optimization of One-Third Tubular Plate Using Finite Element Analysis. *International Current Journal of Engineering and Science (ICJES)*, 4(12), 1-6. Article DOI: https://doi.org/10.47001/ICJES/2025.412001

****

© 2025 ICJES All Rights Reserved